

## RESEARCH AND EDUCATION

# Effect of material and antagonist type on the wear of occlusal devices with different compositions fabricated by using conventional, additive, and subtractive manufacturing

Gökçen Ateş, DDS, PhD,<sup>a</sup> Münir Demirel, DDS, PhD,<sup>b</sup> Mustafa Borga Donmez, DDS, PhD,<sup>c</sup>  
Süleyman Çağatay Dayan, DDS, PhD,<sup>d</sup> and Tonguç Sülün, DDS, PhD<sup>e</sup>

### ABSTRACT

**Statement of problem.** Additive (AM) and subtractive (SM) manufacturing have become popular for fabricating occlusal devices with materials of different chemical compositions. However, knowledge on the effect of material and antagonist type on the wear characteristics of occlusal devices fabricated by using different methods is limited.

**Purpose.** The purpose of this in vitro study was to evaluate the effect of material and antagonist type on the wear of occlusal devices fabricated by using conventional manufacturing, AM, and SM.

**Material and methods.** Two-hundred and forty Ø10×2-mm disk-shaped specimens were fabricated by using heat-polymerized polymethylmethacrylate (control, CM), AM clear device resin fabricated in 3 different orientations (horizontal [AMH], diagonal [AMD], and vertical [AMV]), SM polymethylmethacrylate (SMP), and SM ceramic-reinforced polyetheretherketone (SMB) (n=40). Specimens were then divided into 4 groups based on the antagonists: steatite ceramic (SC); multilayered zirconia (ZR); lithium disilicate (EX); and zirconia-reinforced lithium silicate (ZLS) used for thermomechanical aging (n=10). After aging, the volume loss (mm<sup>3</sup>) and maximum wear depth (µm) were digitally evaluated. Data were analyzed with 2-way analysis of variance and Tukey honestly significant difference tests (α=.05).

**Results.** The interaction between the device material and the antagonist affected volume loss and maximum depth of wear ( $P<.001$ ). AMH had volume loss and depth of wear that was either similar to or higher than those of other materials ( $P\leq.044$ ). When SC was used, CM had higher volume loss and depth of wear than AMV, and, when EX was used, AMD had higher volume loss and depth of wear than SMP ( $P\leq.013$ ). SC and ZR led to higher volume loss of CM and AMH than EX and led to the highest depth of wear for these materials, while ZR also led to the highest volume loss and depth of wear of AMD and AMV ( $P\leq.019$ ). EX led to the lowest volume loss and depth of wear of AMV and SMP and to the lowest depth of wear of AMH ( $P\leq.021$ ). Regardless of the antagonist, SMB had the lowest volume loss and depth of wear ( $P\leq.005$ ).

**Conclusions.** AMH mostly had higher volume loss and depth of wear, while SMB had the lowest volume loss, and its depth of wear was not affected by the tested antagonists. ZR mostly led to higher volume loss and maximum depth of wear, while EX mostly led to lower volume loss and maximum depth of wear of the tested occlusal device materials. (J Prosthet Dent xxx;xxx:xxx-xxx)

Occlusal devices are the most commonly preferred conservative treatment for protecting the masticatory system<sup>1-4</sup> and relieve the symptoms of temporomandibular

disorders.<sup>5,6</sup> These removable appliances have been fabricated with an analog workflow<sup>3-5,7,8</sup> from different materials.<sup>8</sup> However, the fabrication process is time-consuming

This study was funded by Scientific Research Projects Coordination Unit of Istanbul University. Project number: 37954.

The authors declare that they have no known competing financial interests or personal relationships that could have appeared to influence the work reported in this paper.

<sup>a</sup>Postdoctoral Research Associate, Department of Prosthodontics, Faculty of Dentistry, Istanbul University, Istanbul, Turkey; and ITI Scholar, Department of Prosthodontics, University of São Paulo (USP), São Paulo, Brazil.

<sup>b</sup>Assistant Professor, Department of Prosthodontics, Faculty of Dentistry, Biruni University, Istanbul, Turkey.

<sup>c</sup>Associate Professor, Department of Prosthodontics, Faculty of Dentistry, Istinye University, Istanbul, Turkey; and ITI Scholar, Department of Reconstructive Dentistry and Gerodontology, School of Dental Medicine, University of Bern, Bern, Switzerland.

<sup>d</sup>Associate Professor, Program of Dental Technicians, Istanbul University-Cerrahpasa, Istanbul, Turkey.

<sup>e</sup>Professor, Department of Prosthodontics, Faculty of Dentistry, Istanbul University, Istanbul, Turkey.

## Clinical Implications

Ceramic-reinforced polyetheretherketone may be a more suitable alternative than the other tested occlusal device materials for those patients with bruxism given its significantly low volume loss and minimal depth of wear.

and expensive,<sup>9</sup> while the materials present certain shortcomings.<sup>1</sup> Recent advancements in computer-aided design and computer-aided manufacturing (CAD-CAM) technologies have enabled subtractive (SM) and additive manufacturing (AM).<sup>1,5,7,8,10,11</sup> SM allows the fabrication of occlusal devices from prefabricated and standardized CAD-CAM disks in polymethylmethacrylate (PMMA)<sup>5</sup> or polyetheretherketone (PEEK).<sup>1,12</sup> Ceramic-reinforced PEEK (BioHPP; bredent GmbH Co KG) may also be a suitable alternative for those patients with bruxism or those who cannot tolerate a thick occlusal device, as this material has improved mechanical properties.<sup>13</sup> However, the disadvantages of SM<sup>4-6,14</sup> led to the use of AM to fabricate occlusal devices,<sup>15,16</sup> especially with stereolithography (SLA).<sup>4,6,7</sup> Regardless of the technology, however, AM products are anisotropic in relation to the printing direction,<sup>11</sup> making build orientation an essential determinant of their mechanical properties.<sup>16,17</sup>

A successful occlusal device depends on the sustainability of the occlusal contacts as they are applied to reduce the attrition associated with bruxism.<sup>18</sup> Materials used to fabricate an occlusal device should tolerate masticatory forces and be wear-resistant.<sup>6</sup> Wear, defined as gradual material loss,<sup>19,20</sup> is multifactorial and can be classified according to the mechanism of and interaction between materials.<sup>18</sup> Considering the biomechanical nature of the wear, 2-body and 3-body wear tests have been commonly used in dental studies.<sup>21</sup> Two-body wear of occlusal devices, which is associated with nonmasticatory movements such as bruxism, occurs when the material is rubbed away by direct contact of the surfaces, whereas 3-body wear occurs when the surfaces are rubbed away by an intervening slurry of abrasive particles.<sup>18,22</sup>

Even though the 2-body wear of occlusal device materials has been investigated,<sup>5,6,8,12,14,17,23-26</sup> knowledge of the effect of an antagonist on their wear is scarce.<sup>2,26</sup> Also, the effect of build orientation on the wear behavior of AM occlusal devices has not been broadly investigated.<sup>17</sup> Given the trend to fabricate occlusal devices with CAD-CAM technologies and the variability of available materials, a study based on the wear of occlusal device materials in different compositions fabricated by using different methods against different antagonists should further the knowledge of these materials and technologies. Therefore, this study evaluated the wear characteristics of occlusal devices in

materials with different chemical compositions fabricated by using conventional manufacturing, AM, and SM when aged by using 4 different antagonists. The null hypotheses were that the device material and antagonist would not affect the volume loss or maximum wear depth.

## MATERIAL AND METHODS

An overview of this study is shown in Figure 1. A total of 240 disk-shaped specimens were fabricated by using a heat-polymerized PMMA (control, CM, Castdon Transparent; Dreve Dentamid GmbH), an AM clear device resin (AM, Dental LT Clear Resin v2; Formlabs) printed in 3 different orientations (horizontal [0-degree, AMH], diagonal [45-degree, AMD], and vertical [90-degree, AMV]), an SM PMMA (bre.CAM Splint [SMP]; bredent GmbH Co KG), and an SM ceramic-reinforced PEEK (BioHPP [SMB]; bredent GmbH Co KG) (n=40). Each set of specimens was randomly (Excel; Microsoft Corp) divided into 4 subgroups according to the antagonist used for aging (Steatite Ceramic [SC]; SD Mechatronik GmbH, KATANA

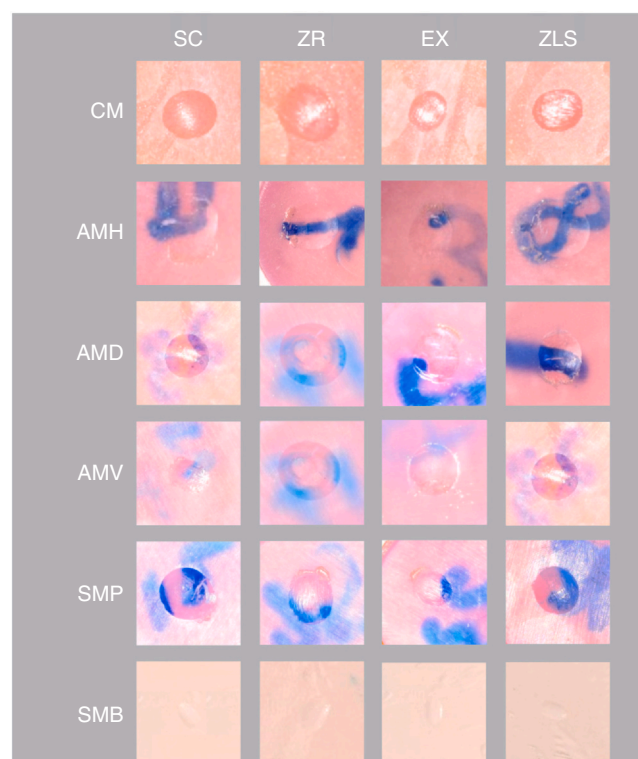


**Figure 1.** Representative image of one specimen from each material-antagonist pair after thermomechanical aging. AMD, additively manufactured resin printed in diagonal orientation; AMH, additively manufactured resin printed in horizontal orientation; AMV, additively manufactured resin printed in vertical orientation; CM, heat-polymerized acrylic resin; EX, lithium disilicate glass-ceramic; SC, steatite ceramic; SMB, ceramic-reinforced polyetheretherketone (BioHPP); SMP, polymethylmethacrylate; ZLS, zirconia-reinforced lithium silicate glass-ceramic; ZR, zirconia.

**Table 1.** List of materials tested

Occlusal Device Material	Chemical Composition	Vickers Hardness
Castdon Transparent (CM)	Polymer: Polymethylmethacrylate copolymer, barbiturate acid derivatives, color pigments Monomer: Methyl methacrylate, quaternary sal ammoniac, stabilizers, catalyst, vulcanizer	188 HV
Dental LT Clear Resin v2 (AM)	Bisphenol A dimethacrylate: 50–70%, urethane dimethacrylate: 25–45%, methacrylate monomer(s): 7–10%, photoinitiator(s): <2%	52 HV (AMH) 55 HV (AMD) 47 HV (AMV)
bre.CAM Splint (SMP) BioHPP (SMB)	Chemoplastic polymethylmethacrylate Modified polyetheretherketone containing 20% ceramic fillers (Particle size: 0.3–0.5 $\mu\text{m}$ )	214 HV 603 HV
Antagonist		
Steatite Ceramic (SC)	SiO <sub>2</sub> : 58–65, MgO: 26–32%, Al <sub>2</sub> O <sub>3</sub> : 3–6%, Na <sub>2</sub> O (for C 220): 1.3%, and BaO (for C 221): 7%	691 HV
Katana STML (ZR) IPS e.max CAD (EX)	ZrO <sub>2</sub> + HfO <sub>2</sub> : $\geq 88$ – $\leq 93\%$ , Y <sub>2</sub> O <sub>3</sub> : 7– $\leq 10\%$ , other oxides: $\leq 2\%$ SiO <sub>2</sub> : 57–80%, Li <sub>2</sub> O: 11–19%, K <sub>2</sub> O: 0–13%, P <sub>2</sub> O <sub>5</sub> : 0–11%, ZrO <sub>2</sub> : 0–8%, ZnO: 0–8%, and coloring oxides: 0–8%	1498 HV 570 HV
Celtra Duo (ZLS)	SiO <sub>2</sub> : 58%, Li <sub>2</sub> O: 18.5%, ZrO <sub>2</sub> : 10%, P <sub>2</sub> O <sub>5</sub> : 5%, CeO <sub>2</sub> : 2%, Al <sub>2</sub> O <sub>3</sub> : 1.9%, and Tb <sub>4</sub> O <sub>7</sub> : %1	630 HV

STML [ZR]; Kuraray Noritake, IPS e.max CAD [EX]; Ivoclar AG, and Celtra Duo [ZLS]; Dentsply Sirona) (n=10) (Table 1). The number of specimens in each group was determined based on a power analysis ( $f=0.26$ ,  $1-\beta=80\%$ ,  $\alpha=.05$ ) that was performed according to the results of a study that reported a minimum meaningful mean difference of 10.8 mm<sup>3</sup> for volume loss and 30.3  $\mu\text{m}$  for maximum depth of wear.<sup>17</sup>

A master disk-shaped standard tessellation language (STL) file ( $\text{\O}10 \times 2.2 \text{ mm}$ ) was designed by using a design software program (Meshmixer v3.5.474; Autodesk Inc). This master STL file was imported into a nesting software program (CEREC inLab CAM v18; Dentsply Sirona) to fabricate SMP and SMB specimens along with wax patterns (Ivory Wax Disc; Dentsply Sirona) to be further processed for CM specimens using a 5-axis milling device (CEREC inLab MCX5; Dentsply Sirona). The burs (Bur 0.5, 1, and 2.5 PMMA; Dentsply Sirona) were changed for new ones after the fabrication of each set of specimens. Wax patterns were then processed as described in a previous article.<sup>5</sup> The master STL file was imported into a nesting software program (Preform v3.6.1; Formlabs) for the fabrication of AM specimens and positioned horizontally (0-degree, AMH), diagonally (45-degree, AMD), or vertically (90-degree, AMV) according to the build platform. Supports were automatically generated (support density of 1.00 and touchpoint size of 0.30 mm), and each orientation was duplicated to generate a total of 10 specimens for each group. Each set of specimen was printed individually by using an SLA-based 3-dimensional (3D) printer (Form 3+; Formlabs) with a 100- $\mu\text{m}$  layer thickness. After fabrication, the AM specimens were cleaned ultrasonically in 99% isopropanol for 15 minutes (Form Wash; Formlabs) followed by soaking in fresh 99% isopropanol for 5 minutes. The specimens were then left to dry for 30 minutes, and the proprietary polymerization unit of the manufacturer (Form Cure; Formlabs) was used to polymerize the specimens for an hour at 60 °C. After polymerization, the supports were removed with a side cutter. One surface of each specimen was wet-ground with silicon carbide abrasive

papers (Struers Labo-Pol 21 #220, #800, and #1200; Struers) and a grinding system (LaboSystem; Struers). All specimens were then highly polished with a pumice slurry followed by a polishing paste (Universal Polishing Paste; Ivoclar AG). The roughness of the specimens was measured 5 times (Marsurf PS1; Mahr), and the values were averaged to ensure that their roughness was similar to or lower than the clinical threshold for bacterial plaque accumulation (0.2  $\mu\text{m}$ ).<sup>1</sup> The final thickness of the specimens was controlled with digital calipers (Model number NB60; Mitutoyo American Corp) to ensure final dimensions of  $\text{\O}10 \times 2 \text{ mm}$ .

Each specimen was embedded in custom-made Teflon molds with autopolymerizing acrylic resin (Technovit 4000; Kulzer GmbH) and digitized by using a 3D profilometer laser scanner (LAS-20; SD Mechatronic) with a horizontal resolution of 0.04 mm<sup>13</sup> and an accuracy of 0.1% over the full scale. Teflon molds were placed in fixed plastic molds to ensure standardized positioning during scanning. All specimens were then stored in distilled water at 37 °C for 24 hours. Before thermomechanical aging, a sphere-shaped STL file, which corresponded to the proprietary SC sphere of the manufacturer of the mastication simulator, was designed (Meshmixer v3.5.474; Autodesk Inc) and processed similarly to the master disk-shaped STL file to mill 6 antagonists from each of the ZR, EX, and ZLS groups. ZR specimens were milled from a 22-mm-thick disk to position the spheres entirely in the enamel layer and to compensate for the sintering shrinkage of approximately 20%. The burs used for milling (Bur 0.5, 1, and 2.5 ZrO<sub>2</sub> DC; Dentsply Sirona for ZR and Diamond 0.6, Diamond 1.2, Diamond 1.4, and Diamond 2.2; Dentsply Sirona for EX and ZLS) were changed between each set of antagonists. After fabrication, ZR specimens were sintered (inFire HTC speed; Dentsply Sirona) and EX specimens were crystallized (Programat P300; Ivoclar AG) by following their respective manufacturer's recommendations. No further adjustments were made to the antagonists. The specimens were subjected to thermomechanical aging (Chewing Simulator CS-4.8; SD Mechatronic GmbH) in distilled water under a

50-N load<sup>2,5,6,14,18,25</sup> with a frequency of 1.6 Hz, a vertical movement of 2 mm, and a lateral movement of 0.7 mm for 120 000 cycles (5 °C–55 °C, dwell time 30 seconds) to simulate 6 months of intraoral use<sup>1,5</sup> (Fig. 1), and the process was randomized by using a software program (Excel; Microsoft Corp). One antagonist was used for each material subgroup, resulting in a total of 24 antagonists.

After thermomechanical aging, all specimens were digitized by using the same laser scanner, and a metrology-grade 3D analysis software program (Geomagic Control X 2020.1; 3D Systems) was used to superimpose the after thermomechanical aging datasets over their respective reference before thermomechanical aging datasets by using the iterative closest point best-fit alignment. Color maps that would facilitate the analysis of worn areas were generated by using the "3D Compare tool" of the software program with maximum and minimum deviation values set at +100 µm and -100 µm, and the tolerance range was set at +10 µm and 10 µm (Fig. 2). To calculate the volumetric difference of the worn area between 2 data sets, the worn area was manually cropped on both data sets by using the "measurement tool-volume inspection tool-enclosed volume" feature, which automatically calculated the volume of the cropped area. The absolute volume difference was then determined by calculating the difference between these

values (Fig. 3). To measure the maximum wear depth, a plane that encompassed the worn area was generated. The maximum wear depth was defined as the highest distance between this plane and the worn area on the z-axis. To ensure that the selected point on the worn area was at the deepest point, a buccopalatal cross-section that equally divided the worn area was also generated (Fig. 4).<sup>27</sup>

Given that the hardness of the tested materials was mostly not disclosed by their manufacturers and that those materials with internal hardness data were evaluated by using different test methods, 3 additional specimens from each occlusal device material and each antagonist (Ø10×2 mm) were prepared to measure their Vickers hardness. A load of 9.81 N was applied for 15 seconds with a Vickers hardness tester (Falcon 400; Innovatest), and 3 readings that were 0.5 mm apart from each other were made per specimen.<sup>28–30</sup> The arithmetic mean of 9 readings were calculated per material (Table 1).

The Shapiro-Wilk test was used to evaluate the distribution of data, which yielded normal distribution. Therefore, 2-way analysis of variance and Tukey honestly significant difference tests were performed with a statistical analysis software program (IBM SPSS Statistics, v23; IBM Corp) to analyze the volume loss and maximum wear depth data ( $\alpha=.05$ ).

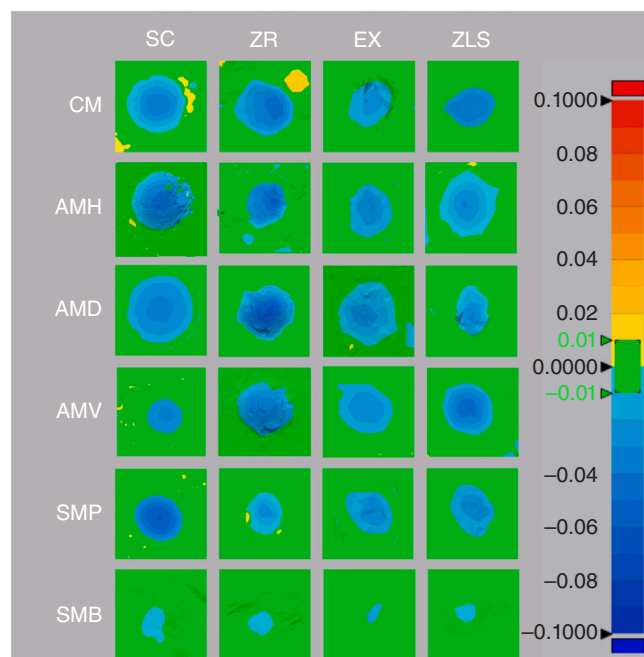


**Figure 2.** Color maps generated after superimpositions for each material-antagonist pair. AMD, additively manufactured resin printed in diagonal orientation; AMH, additively manufactured resin printed in horizontal orientation; AMV, additively manufactured resin printed in vertical orientation; CM, heat-polymerized acrylic resin; EX, lithium disilicate glass-ceramic; SC, steatite ceramic; SMB, ceramic-reinforced polyetheretherketone (BioHPP); SMP, polymethylmethacrylate; ZLS, zirconia-reinforced lithium silicate glass-ceramic; ZR, zirconia.

## RESULTS

The device material, antagonist, and interaction between the main factors significantly affected volume loss ( $P<.001$ ) (Table 2). When SC was used, SMB had the lowest volume loss, AMH and CM had higher volume loss than AMV, and AMH also had higher volume loss than AMD ( $P\le.040$ ). When ZR was used, SMB had the lowest volume loss, which was followed by SMP ( $P\le.010$ ). When EX was used, SMB had the lowest volume loss, AMH and AMD had higher volume loss than SMP, and AMH also had higher volume loss than AMV ( $P\le.013$ ). When ZLS was used, SMB had the lowest volume loss and AMH had a higher volume loss than CM ( $P\le.044$ ). For CM, SC and ZR antagonists led to the highest volume loss ( $P<.001$ ). For AMH, ZR led to higher volume loss than EX and ZLS ( $P\le.030$ ), while SC also led to higher volume loss than EX ( $P<.001$ ). For AMD, ZR led to the highest volume loss ( $P\le.002$ ). For AMV, ZR led to the highest, and EX led to the lowest volume loss ( $P\le.020$ ). For SMP, EX led to the lowest volume loss ( $P<.001$ ). For SMB, SC led to higher volume loss than ZLS ( $P=.026$ ) (Table 3).

The device material, antagonist, and interaction between the main factors significantly affected the maximum depth of wear ( $P<.001$ ) (Table 2). When SC was used, SMB had the lowest wear depth, AMH and CM



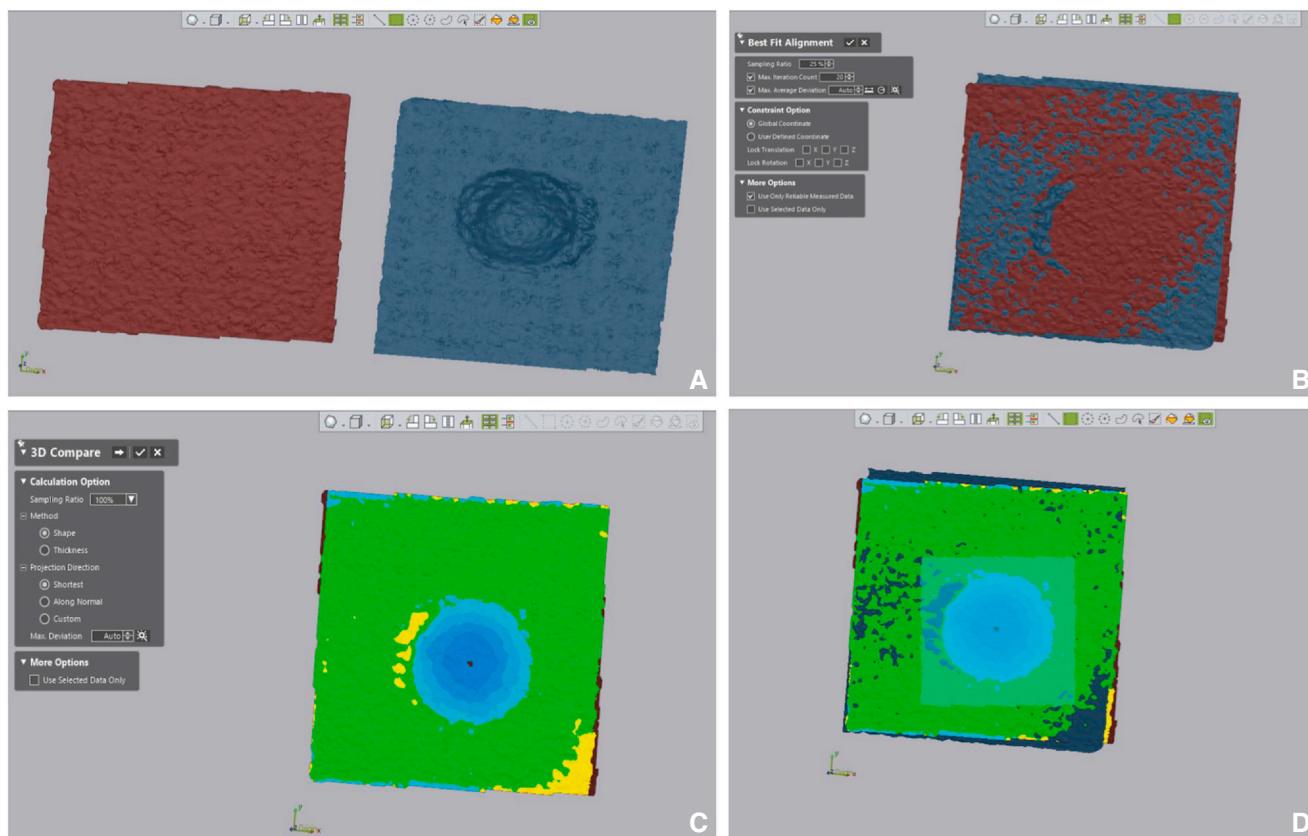


**Figure 3.** Superimposition of after thermomechanical aging data (blue) over before thermomechanical aging data (red). A, Before and after thermomechanical aging data before superimposition. B, Before and after thermomechanical aging data after superimposition by using best-fit alignment. C, Color map generated after superimposition. D, Manual selection of worn area on both standard tessellation language files.

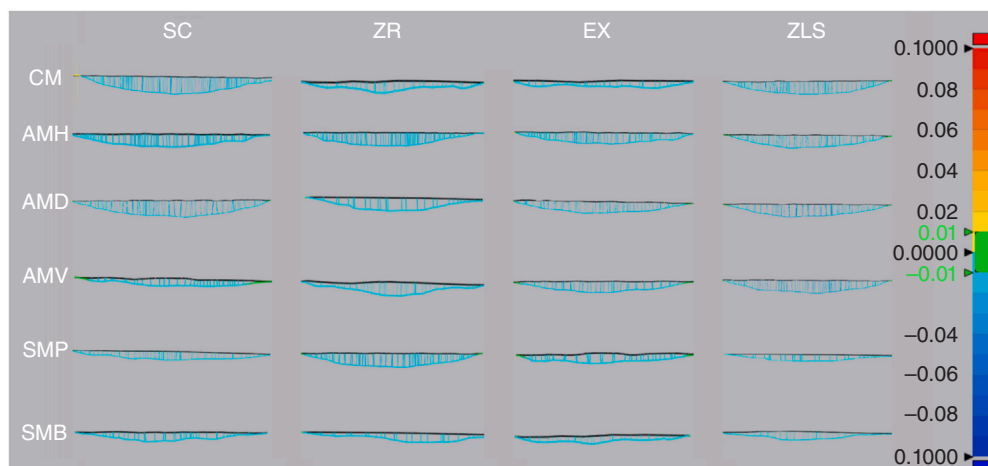


**Figure 4.** Representative image of worn area for each material-antagonist pair after superimposition. AMD, additively manufactured resin printed in diagonal orientation; AMH, additively manufactured resin printed in horizontal orientation; AMV, additively manufactured resin printed in vertical orientation; CM, heat-polymerized acrylic resin; EX, lithium disilicate glass-ceramic; SC, steatite ceramic; SMB, ceramic-reinforced polyetheretherketone (BioHPP); SMP, polymethylmethacrylate; ZLS, zirconia-reinforced lithium silicate glass-ceramic; ZR, zirconia.

had higher wear depth than AMV, and AMH had higher values than SMP ( $P \leq .036$ ). When ZR was used, SMB had the lowest wear depth followed by SMP ( $P \leq .008$ ). When EX was used, SMB had the lowest values, AMH and

AMD had higher values than SMP, and AMH also had higher values than SMP ( $P \leq .013$ ). When ZLS was used, SMB had the lowest wear depth ( $P < .001$ ). For CM, ZR and SC led to the highest wear depth ( $P < .001$ ). For

**Table 2.** Results of two-way analysis of variance tests for volume loss and maximum depth of wear

	Volume Loss					Maximum Depth of Wear				
	df	Mean Square	F	P	Partial Eta Squared	df	Mean Square	F	P	Partial Eta Squared
Material	5	0.461	95.345	<.001	.688	5	0.029	96.923	<.001	.692
Antagonist	3	0.427	88.298	<.001	.551	3	0.027	88.563	<.001	.552
Material × Antagonist	15	0.037	7.608	<.001	.346	15	0.002	7.559	<.001	.344

**Table 3.** Mean ± standard deviation (95% confidence interval) volume loss (mm<sup>3</sup>) of each material-antagonist pair

	SC	ZR	EX	ZLS
CM	0.45 ± 0.08 <sup>Bcd</sup> (0.40–0.50)	0.51 ± 0.05 <sup>Bc</sup> (0.48–0.54)	0.25 ± 0.07 <sup>Abcd</sup> (0.20–0.30)	0.29 ± 0.11 <sup>Ab</sup> (0.21–0.37)
AMH	0.46 ± 0.07 <sup>Bcd</sup> (0.41–0.51)	0.48 ± 0.04 <sup>Cc</sup> (0.45–0.50)	0.31 ± 0.06 <sup>Ad</sup> (0.26–0.35)	0.40 ± 0.04 <sup>Bb</sup> (0.37–0.43)
AMD	0.36 ± 0.09 <sup>Abc</sup> (0.29–0.42)	0.51 ± 0.12 <sup>Bc</sup> (0.44–0.60)	0.27 ± 0.05 <sup>Acd</sup> (0.23–0.30)	0.37 ± 0.07 <sup>Ab</sup> (0.32–0.42)
AMV	0.33 ± 0.11 <sup>Bb</sup> (0.26–0.41)	0.56 ± 0.08 <sup>Cc</sup> (0.50–0.62)	0.20 ± 0.02 <sup>Abc</sup> (0.19–0.22)	0.39 ± 0.13 <sup>Bb</sup> (0.30–0.48)
SMP	0.37 ± 0.04 <sup>Bbcd</sup> (0.34–0.40)	0.36 ± 0.10 <sup>Bb</sup> (0.29–0.42)	0.19 ± 0.03 <sup>Ab</sup> (0.17–0.21)	0.32 ± 0.06 <sup>Bb</sup> (0.28–0.37)
SMB	0.13 ± 0.03 <sup>Ba</sup> (0.11–0.15)	0.12 ± 0.02 <sup>ABa</sup> (0.11–0.14)	0.11 ± 0.01 <sup>ABa</sup> (0.10–0.12)	0.11 ± 0.01 <sup>ABa</sup> (0.10–0.11)

\*Different superscript uppercase letters indicate significant differences in rows, while different superscript lowercase letters indicate significant differences in columns ( $P < .05$ )

AMH, EX led to the lowest, and SC and ZR led to the highest wear depth ( $P \leq .019$ ). For AMD, ZR led to the highest values ( $P \leq .003$ ). For AMV, EX led to the lowest and ZR led to higher values than those of the remaining materials ( $P \leq .021$ ), other than SC ( $P \leq .001$ ). For SMP, EX led to the lowest values ( $P < .001$ ), while antagonist type did not affect the wear depth of SMB ( $P \geq .058$ ) (Table 4).

## DISCUSSION

The present study investigated the wear behavior of occlusal device materials with different chemical compositions fabricated by using conventional, AM, and subtractive manufacturing with different antagonists. The device material and the antagonist affected the volume loss and maximum wear depth. Therefore, the null hypotheses that the device material and antagonist would not affect the volume loss or maximum wear depth were rejected.

Regardless of the antagonist, SMB had the lowest volume loss and wear depth among the tested occlusal device materials, whereas AMH mostly had higher volume loss and wear depth than the remaining materials. Except for SMB, the tested occlusal device materials mostly had higher volume loss and wear depth when ZR

antagonists were used and mostly had lower volume loss and wear depth when EX antagonists were used. A possible explanation of these differences may be the hardness of the tested materials. The tested occlusal device materials and antagonists have distinct chemical compositions, which affect their hardness and resistance to wear.<sup>27</sup> Even though a comparison among the hardness of tested occlusal device materials and antagonists was not an aim of the present study, the Vickers hardness measurements corroborated this interpretation. The manufacturer of the tested AM resin recommends either horizontal orientation or an angle up to 40 degrees during manufacturing.<sup>31</sup> Even though AMH and AMD groups replicated these recommendations, AMH had higher volume loss and wear depth than either or both of the AM groups when SC and EX were used. The authors think the square-shaped geometry of the specimens could be associated with these results, as a more complex structure, like an actual occlusal device, may have different wear characteristics.

Consistent with the volume loss and wear depth results, SMB had the smallest and the shallowest worn area among the tested materials, regardless of the antagonist. Therefore, SMB may be a more suitable alternative to other tested occlusal device materials for those patients with severe bruxism when fabricated in the

**Table 4.** Mean ± standard deviation (95% confidence interval) maximum depth of wear (μm) of each material-antagonist pair

	SC	ZR	EX	ZLS
CM	0.11 ± 0.02 <sup>Bcd</sup> (0.10–0.13)	0.13 ± 0.01 <sup>Bc</sup> (0.12–0.14)	0.06 ± 0.02 <sup>Abcd</sup> (0.05–0.07)	0.07 ± 0.03 <sup>Ab</sup> (0.05–0.09)
AMH	0.12 ± 0.02 <sup>Cd</sup> (0.11–0.13)	0.12 ± 0.01 <sup>Cc</sup> (0.11–0.13)	0.08 ± 0.02 <sup>Ad</sup> (0.06–0.09)	0.10 ± 0.01 <sup>Bb</sup> (0.10–0.10)
AMD	0.09 ± 0.02 <sup>Abcd</sup> (0.08–0.11)	0.13 ± 0.03 <sup>Bc</sup> (0.11–0.15)	0.07 ± 0.02 <sup>Acd</sup> (0.06–0.08)	0.09 ± 0.02 <sup>Ab</sup> (0.08–0.10)
AMV	0.08 ± 0.03 <sup>Bb</sup> (0.07–0.10)	0.14 ± 0.02 <sup>Cc</sup> (0.13–0.15)	0.05 ± 0.01 <sup>Abc</sup> (0.05–0.05)	0.10 ± 0.03 <sup>Bb</sup> (0.07–0.12)
SMP	0.09 ± 0.01 <sup>Bbc</sup> (0.08–0.10)	0.09 ± 0.02 <sup>Bb</sup> (0.07–0.11)	0.05 ± 0.01 <sup>Ab</sup> (0.04–0.05)	0.08 ± 0.02 <sup>Bb</sup> (0.07–0.09)
SMB	0.03 ± 0.01 <sup>Aa</sup> (0.03–0.04)	0.03 ± 0.01 <sup>Aa</sup> (0.03–0.03)	0.03 ± 0.01 <sup>Aa</sup> (0.03–0.03)	0.03 ± 0.01 <sup>Aa</sup> (0.03–0.03)

\*Different superscript uppercase letters indicate significant differences in rows, while different superscript lowercase letters indicate significant differences in columns ( $P < .05$ )

same thickness. In addition, patients with a gagging reflex may benefit from SMB, as reduced material thickness may not be associated with premature failure. SMP also mostly had color maps that were either smaller or shallower than the remaining materials, which may indicate the possible effect of the manufacturing method on wear as the materials other than SMB were also acrylate-based. SM materials were fabricated under standardized conditions<sup>6,10</sup>; therefore, SMP and SMB may have a higher degree of conversion that leads to more favorable mechanical properties. The remaining materials had color maps with dominant darker blue shades, which represent greater wear, when ZR was used. Other than AMV, SC led to a worn area that was either deeper or wider for CM, AMH, and AMD, which was also consistent with the volume loss and wear depth data.

The authors are unaware of previous studies on the wear of the tested materials. In addition, methodological differences in thermomechanical aging process complicate the comparison of the results with previous in vitro studies<sup>5,6,8,14,17,23–26</sup> on the wear of CAD-CAM manufactured occlusal devices. Nevertheless, the effect of different antagonists has been investigated.<sup>2,26</sup> Reyes-Sevilla et al<sup>26</sup> reported that AM occlusal devices had a lower wear rate than those manufactured conventionally and with SM, while different antagonists affected the wear rate. Yildiz Domanic et al<sup>2</sup> reported that pressed lithium disilicate led to higher volume loss than enamel and translucent zirconia while using conventionally manufactured occlusal device materials with different compositions. Another study concluded that specimens manufactured at 0-degrees had higher wear resistance than those manufactured at 45 degrees or 90 degrees.<sup>17</sup>

The laser scanner<sup>2,5,25</sup> and the software program<sup>2,6,17</sup> used in the present study have been previously used to investigate the wear characteristics of occlusal device materials. The iterative closest point-based best-fit algorithm was chosen as the tested specimens did not have specific features that are present on an actual occlusal device, which may have facilitated best-fit algorithms such as landmark-based alignment or reference base-fit. The methodology to calculate the volume loss and maximum wear depth has also been used in a recent study on the wear of AM and SM resin-based materials.<sup>27</sup> Considering these aspects, the authors consider the methodology of the present study to be justified and reliable.

As in previous studies,<sup>8,14,23,24</sup> steatite was chosen because of its standardized geometry, which also standardized the geometry of the remaining antagonists. However, the absence of human enamel is a limitation. All materials were limited to one brand, and fabrication processes were performed by using one milling unit and one 3D printer. AM specimens were postprocessed following the manufacturer's recommendations; however,

a recent study has reported that the atmospheric condition of polymerization may affect wear behavior.<sup>24</sup> Also, other printing parameters such as layer thickness were not investigated. All specimens were polished using a standardized laboratory procedure to have a clinically acceptable surface roughness; however, different polishing methods may affect the surface characteristics and wear behavior. The magnitude of volume loss and wear depth values might have been amplified, given that the antagonists were not polished or glazed to generate a worst-case scenario. The thermomechanical aging process did not involve saliva, and the temperature fluctuation might have deteriorated the mechanical properties and exacerbated the results, as occlusal devices are not used during beverage or food consumption. Another limitation was that the wear of the antagonists and the surface roughness of the tested materials during or after the 2-body wear test were not investigated. Future studies should evaluate how the 2-body and 3-body wear of tested occlusal device materials affect their mechanical and optical properties, with more detailed analyses of wear mechanisms and parameters such as coefficient of friction and Hertzian contact pressure to elaborate their limitations.

## CONCLUSIONS

Based on the findings of this in vitro study, the following conclusions were drawn:

1. Regardless of the antagonist, ceramic-reinforced polyetheretherketone had the lowest volume loss and depth of wear, while the tested antagonists did not affect its depth of wear. The additively manufactured resin fabricated with the horizontal orientation mostly had higher volume loss and depth of wear.
2. Among the tested antagonists, multilayered zirconia mostly led to higher and lithium disilicate mostly led to lower volume loss and depth of wear.

## REFERENCES

1. Benli M, Eker Gümüş B, Kahraman Y, et al. Surface roughness and wear behavior of occlusal splint materials made of contemporary and high-performance polymers. *Odontology*. 2020;108:240–250.
2. Yildiz Domanic K, Aslan YU, Ozkan Y. Two-body wear of occlusal splint materials against different antagonists. *BMC Oral Health*. 2020;20:174.
3. Perea-Lowery L, Gibreel M, Vallittu PK, Lassila L. Evaluation of the mechanical properties and degree of conversion of 3D printed splint material. *J Mech Behav Biomed Mater*. 2020;115:104254.
4. Marcel R, Reinhard H, Andreas K. Accuracy of CAD/CAM-fabricated bite splints: Milling vs 3D printing. *Clin Oral Invest*. 2020;24:4607–4615.
5. Lutz AM, Hampe R, Roos M, et al. Fracture resistance and 2-body wear of 3-dimensional-printed occlusal devices. *J Prosthet Dent*. 2019;121:166–172.
6. Wesemann C, Spies BC, Sterzenbach G, et al. Polymers for conventional, subtractive, and additive manufacturing of occlusal devices differ in hardness and flexural properties but not in wear resistance. *Dent Mater*. 2021;37:432–442.

7. Prpic V, Slacanin I, Schauperl Z, et al. A study of the flexural strength and surface hardness of different materials and technologies for occlusal device fabrication. *J Prosthet Dent*. 2019;121:955–959.
8. Huettig F, Kustermann A, Kuscü E, et al. Polishability and wear resistance of splint material for oral appliances produced with conventional, subtractive, and additive manufacturing. *J Mech Behav Biomed Mater*. 2017;75:175–179.
9. Berli C, Thieringer FM, Sharma N, et al. Comparing the mechanical properties of pressed, milled, and 3D-printed resins for occlusal devices. *J Prosthet Dent*. 2020;124:780–786.
10. Wesemann C, Spies BC, Schaefer D, et al. Accuracy and its impact on fit of injection molded, milled and additively manufactured occlusal splints. *J Mech Behav Biomed Mater*. 2021;114:104179.
11. Väyrynen VO, Tanner J, Vallittu PK. The anisotropy of the flexural properties of an occlusal device material processed by stereolithography. *J Prosthet Dent*. 2016;116:811–817.
12. Wang S, Li Z, Ye H, et al. Preliminary clinical evaluation of traditional and a new digital PEEK occlusal splints for the management of sleep bruxism. *J Oral Rehabil*. 2020;47:1530–1537.
13. Diken Türksayar AA, Hisarbeyli D, Seçkin Kelten Ö, Bulucu NB. Wear behavior of current computer-aided design and computer-aided manufacturing composites and reinforced high performance polymers: An in vitro study. *J Esthet Restor Dent*. 2022;34:527–533.
14. Rosentritt M, Huber C, Strasser T, Schmid A. Investigating the mechanical and optical properties of novel Urethandimethacrylate (UDMA) and Urethanmethacrylate (UMA) based rapid prototyping materials. *Dent Mater*. 2021;37:1584–1591.
15. Strub JR, Rekow ED, Witkowski S. Computer-aided design and fabrication of dental restorations: Current systems and future possibilities. *J Am Dent Assoc*. 2006;137:1289–1296.
16. Shim JS, Kim JE, Jeong SH, et al. Printing accuracy, mechanical properties, surface characteristics, and microbial adhesion of 3D-printed resins with various printing orientations. *J Prosthet Dent*. 2020;124:468–475.
17. Grymak A, Waddell JN, Aarts JM, et al. Evaluation of wear behaviour of various occlusal splint materials and manufacturing processes. *J Mech Behav Biomed Mater*. 2022;126:105053.
18. Kurt H, Erdelt KJ, Cilingir A, et al. Two-body wear of occlusal splint materials. *J Oral Rehabil*. 2012;39:584–590.
19. D'Arcangelo C, Vanini L, Rondoni GD, De Angelis F. Wear properties of dental ceramics and porcelains compared with human enamel. *J Prosthet Dent*. 2016;115:350–355.
20. Bayraktar ET, Türkmen C, Atalı PY, et al. Evaluation of correlation between wear resistance and microhardness of resin based CAD/CAM blocks. *European Journal of Research in Dentistry*. 2020;4:25–30.
21. Grymak A, Aarts JM, Ma S, et al. Wear behavior of occlusal splint materials manufactured by various methods: A systematic review. *J Prosthodont*. 2022;31:472–487.
22. Lambrechts P, Debels E, Van Landuyt K, et al. How to simulate wear? Overview of existing methods. *Dent Mater*. 2006;22:693–701.
23. Gibrel M, Perea-Lowery L, Vallittu PK, et al. Two-body wear and surface hardness of occlusal splint materials. *Dent Mater J*. 2022;41:916–922.
24. Wada J, Wada K, Garoushi S, et al. Effect of 3D printing system and post-curing atmosphere on micro- and nano-wear of additive-manufactured occlusal splint materials. *J Mech Behav Biomed Mater*. 2023;142:105799.
25. Schmeiser F, Baumert U, Stawarczyk B. Two-body wear of occlusal splint materials from subtractive computer-aided manufacturing and three-dimensional printing. *Clin Oral Investig*. 2022;26:5857–5866.
26. Reyes-Sevilla M, Kuijs RH, Werner A, et al. Comparison of wear between occlusal splint materials and resin composite materials. *J Oral Rehabil*. 2018;45:539–544.
27. Lawson NC, Bansal R, Burgess JO. Wear, strength, modulus and hardness of CAD/CAM restorative materials. *Dent Mater*. 2016;32:e275–e283.
28. Wada J, Wada K, Garoushi S, et al. Effect of 3D printing system and post-curing atmosphere on micro- and nano-wear of additive-manufactured occlusal splint materials. *J Mech Behav Biomed Mater*. 2023;142:105799.
29. Donmez MB, Olcay EO, Demirel M. Influence of coloring liquid immersion on flexural strength, Vickers hardness, and color of zirconia. *J Prosthet Dent*. 2021;126:589. e1–e6.
30. Diken Türksayar AA, Demirel M, Donmez MB, et al. Comparison of wear and fracture resistance of additively and subtractively manufactured screw-retained, implant-supported crowns. *J Prosthet Dent* 2023.
31. Formlabs. Instructions for Use. Dental LT Clear V2 Resin. Available at: (<https://media.formlabs.com/m/a4f5cb31bb87549/original/Dental-LT-Clear-V2-Resin-Instructions-for-Use.pdf>). Accessed on October 3, 2023.

**Corresponding author:**

Dr Mustafa Borga Dönmez  
 Department of Reconstructive Dentistry and Gerodontology  
 School of Dental Medicine  
 University of Bern  
 Freiburgstrasse 7  
 Bern 3010  
 SWITZERLAND  
 Email: [mustafa-borga.doenmez@unibe.ch](mailto:mustafa-borga.doenmez@unibe.ch)

**CRediT authorship contribution statement**

**Gökçen Ateş:** Investigation, methodology. **Münir Demirel:** Investigation, methodology. **Mustafa Borga Donmez:** Writing - original draft, Critical revision of article. **Süleyman Çağatay Dayan:** Formal analysis. **Tonguç Sülün:** Project administration, Supervision, Critical revision.

Copyright © 2024 The Authors. Published by Elsevier Inc. on behalf of the Editorial Council of *The Journal of Prosthetic Dentistry*. This is an open access article under the CC BY license (<http://creativecommons.org/licenses/by/4.0/>). <https://doi.org/10.1016/j.prosdent.2024.03.026>